Sliter, S. Stein, Eds. (Monograph 77, American Geophysical Union, Washington, DC, 1993), pp. 233–261.
2. M. F. Coffin and O. Eldholm, *Rev. Geophys.* **32**, 1 (1994).
3. W. J. Morgan, in *The Sea*, C. Emiliani, Ed. (Wiley, New York, 1981), vol. 7, pp. 443–487.
4. M. A. Richards, R. A. Duncan, V. E. Courtillot, *Science* **246**, 103 (1989).
5. R. White and D. P. McKenzie, *J. Geophys. Res.* **94**, 7685 (1989).
6. I. H. Campbell and R. W. Griffiths, *Earth Planet. Sci. Lett.* **99**, 79 (1990).
7. J. A. Whitehead and D. S. Luther, *J. Geophys. Res.* **80**, 705 (1975).
8. M. L. G. Tejada, J. J. Mahoney, R. A. Duncan, M. P. Hawkins, in preparation.
9. R. A. Duncan, *Proc. Ocean Drilling Program Sci. Results* **121**, 507 (1991); M. Pringle and M. Storey, in preparation.
10. W. W. Sager and H.-C. Han, *Nature* **364**, 610 (1993).
11. L. W. Kroenke and W. W. Sager, *Eos* **74** (fall suppl.), 555 (1993).
12. M. S. Pringle and G. B. Dalrymple, in *The Mesozoic Pacific: Geology, Tectonics, and Volcanism*, M. Pringle, W. Sager, W. Sliter, S. Stein, Eds. (Monograph 77, American Geophysical Union, Washington, DC, 1993), pp. 263–277.
13. P. R. Renne *et al.*, *Science* **258**, 975 (1992); A. K. Baksi, R. V. Fodor, E. Farrar, *Eos* **72** (spring suppl.), 300 (1991); S. Turner, M. Regelous, S. Kelley, C. Hawkesworth, M. Mantovani, *Earth Planet. Sci. Lett.* **121**, 333 (1994).
14. J. M. O'Connor and R. A. Duncan, *J. Geophys. Res.* **95**, 17475 (1990).
15. P. R. Hooper, J. Rehacek, R. A. Duncan, J. S. Marsh, A. R. Duncan, *Eos* **74** (fall suppl.), 553 (1993); R. A. Duncan, personal communication.
16. M. Storey *et al.*, unpublished results.
17. R. W. Kent, M. Storey, A. D. Saunders, *Geology* **20**, 891 (1992).
18. D. K. Rea and T. L. Vallier, *Geol. Soc. Am. Bull.* **94**, 1430 (1987).
19. P. Olson and I. S. Nam, *J. Geophys. Res.* **91**, 7181 (1986); R. W. Griffiths and I. H. Campbell, *ibid.* **96**, 18295 (1991).
20. J. N. Skilbeck and J. A. Whitehead, *Nature* **272**, 499 (1978); P. Olson and H. Singer, *J. Fluid Mech.* **158**, 511 (1985).
21. P. Olson and U. Christensen, *J. Geophys. Res.* **91**, 6367 (1986); D. R. Scott, D. J. Stevenson, J. A. Whitehead, *Nature* **319**, 759 (1986); K. R. Helfrich and J. A. Whitehead, *Geophys. Astrophys. Fluid Dyn.* **51**, 35 (1990).
22. B. H. Hager, *J. Geophys. Res.* **89**, 6003 (1984); S. D. King and G. Masters, *Geophys. Res. Lett.* **19**, 1551 (1992).
23. The laboratory experiments suggest that rather than immediately separating from the conduit, the accelerating plume head causes the conduit to be stretched into an extremely thin filament (Fig. 2). The fluid in the lower, unthinned portion of the conduit rises through this filament by forming an upward propagating bore; the head of the bore inflates until it is soon indistinguishable from another plume head. Typically, the filament diffuses away before the bore moves a large distance, causing the bore to become a genuine diapir. See also the numerical models of plumes interacting with a viscosity transitions [for example, L. H. Kellogg, *Geophys. Res. Lett.* **18**, 865 (1991); P. E. van Keken, D. A. Yuen, A. P. van den Berg, *Earth. Planet. Sci. Lett.* **112**, 179 (1992); *Geophys. Res. Lett.* **20**, 1927 (1993); M. Manga, H. A. Stone, R. J. O'Connell, *J. Geophys. Res.* **98**, 19979 (1993)].
24. P. Olson, in *Magma Transport and Storage*, M. P. Ryan, Ed. (Wiley, New York, 1990), pp. 33–51.
25. If the volume of the conduit is negligible, then the radius of the first plume head upon reaching the interface between the upper mantle and the lower mantle is

$$R = R_0(1 + 5D_\ell/R_0)^{1/5}$$

where

$$R_0 = \left(\frac{3\mu_\ell Q}{4\pi\Delta\rho g}\right)^{1/4}$$

is the radius of the plume head upon detachment from the *D″* layer [see (*24*), equation 15]. Because we expect $D_\ell \gg R_0$, we can use the expression for R to approximate the volume flux in the conduit as

$$Q = \frac{4\pi\Delta\rho g}{15D_\ell\mu_\ell}R^5$$

26. N. M. Ribe and D. P. de Valpine, *Geophys. Res. Lett.* **21**, 1507 (1994).
27. J. X. Mitrovica and W. R. Peltier, *ibid.* **19**, 1185 (1992).
28. For simplicity, we neglect the effects of the endothermic phase change at the 660-km discontinuity [see E. Ito and E. Takahashi, *J. Geophys. Res.* **94**, 10637 (1989); E. Ito, M. Akaogi, L. Topor, A. Navrotsky, *Science* **249**, 1275 (1990)]. In fact, this phase transition should impede penetration of the second plume head into the upper mantle [see M. Liu, D. A. Yuen, W. Zhao, S. Honda, *Science* **252**, 1836 (1991); T. Nakakuki, H. Sato, H. Fujimoto, *Earth Planet. Sci. Lett.* **121**, 369 (1994)]. Moreover, we again must use R = 363 km (that is, an R based on the volume of all the plume head material forming the Ontong Java Plateau), which leads to underestimates of the formation and transit times for the second plume head. The time necessary for the second plume head to inflate and begin ascent is

$$t_d = \left(\frac{4\pi\mu_u^3}{3Q\Delta\rho^3 g^3}\right)^{1/4} \approx 1.2 \text{ million years}$$

(using, as a conservative estimate, $\mu_\ell = 3 \times 10^{22}$ Pa-s to determine Q) (*7*, *24*). See (*25*) on the determination of Q. The time for this second plume head to rise across the upper mantle is

$$t_r = \frac{4\pi R_1^3}{3Q}[(1 + 5fD_u/R_1)^{3/5} - 1]$$

where

$$R_1 = \left(\frac{3\mu_u Q}{4\pi\Delta\rho g}\right)^{1/4}$$

is the radius of the second plume head when it begins its ascent and f is the fraction of the upper mantle left for the second plume head to traverse. If μ_u/μ_ℓ is sufficiently small, then f is of order of magnitude 1 (that is, separation of the first plume head occurs quickly and near the 660-km boundary); however, f can be as low as 1/3 before it has an influence on t_r. The expression for t_r is slightly more general than that given by Olson (*24*) but follows from the same derivation. The volume of the second plume head upon reaching the base of the lithosphere is

$$\text{volume} = \frac{4\pi R_1^3}{3}(1 + 5D_u/R_1)^{3/5}$$

or

$$= Qt_r + \frac{4\pi}{3}R_1^3$$

29. Increasing μ_ℓ (for example, to 10^{23} Pa-s) or decreasing R (to reflect only a part of the net Ontong Java plume head volume) would enhance the likelihood that the first plume head separates from the conduit (U/V_{max} would increase) and would lengthen the time delay between eruptive events; these same adjustments would also diminish the volume of the second plume head. Perhaps more importantly, the addition of the endothermic phase change (*28*) would undoubtedly make separation of the first plume head more probable [see in particular Liu *et al.* in (*28*)], lengthen the delay time between arrival of the plume heads, and increase the volume of the second plume head. However, if the conduit flux Q is not sufficiently large, the phase change may preclude the penetration of the second plume head into the upper mantle altogether [see Liu *et al.* in (*28*)].
30. We thank A. Kelly for assistance with the laboratory experiments, S. A. Weinstein and L. W. Kroenke for useful discussions, and D. A. Yuen and J. A. Whitehead for insightful reviews. This work was supported by the National Science Foundation (grants EAR-9303402 and EAR-9104897). School of Ocean and Earth Science and Technology, University of Hawaii, contribution number 3663.

16 June 1994; accepted 28 September 1994

Activation and Regeneration of Rhodopsin in the Insect Visual Cycle

Alexander Kiselev and Sriram Subramaniam*

Light absorption by rhodopsin generates metarhodopsin, which activates heterotrimeric guanine nucleotide–binding proteins (G proteins) in photoreceptor cells of vertebrates and invertebrates. In contrast to vertebrate metarhodopsins, most invertebrate metarhodopsins are thermally stable and regenerate rhodopsin by absorption of a second photon. In experiments with Rh1 *Drosophila* rhodopsin, the thermal stability of metarhodopsin was found not to be an intrinsic property of the visual pigment but a consequence of its interaction with arrestin (49 kilodaltons). The stabilization of metarhodopsin resulted in a large decrease in the efficiency of G protein activation. Light absorption by thermally stable metarhodopsin initially regenerated an inactive rhodopsin-like intermediate, which was subsequently converted in the dark to active rhodopsin. The accumulation of inactive rhodopsin at higher light levels may represent a mechanism for gain regulation in the insect visual cycle.

In both vertebrates and invertebrates, light absorption by rhodopsin triggers activation of G proteins in the photoreceptor cell (*1*, *2*). In vertebrates, the intermediate (metarhodopsin II) that activates G proteins is thermally unstable and decays eventually into all-*trans* retinal and opsin (*3*). Rhodopsin is subsequently regenerated by the recombination of 11-*cis* retinal with opsin (*4*). In contrast, in most invertebrates, the intermediate (metarhodopsin) believed to activate photoreceptor G proteins is thermally stable (*5*, *6*). In invertebrates, rhodopsin is regenerated by illuminating metarhodopsin (*5*, *7*,

Department of Biological Chemistry, Johns Hopkins University School of Medicine, Baltimore, MD 21205, USA.

*To whom correspondence should be addressed.

8). The invertebrate visual cycle therefore requires photon absorption to drive both the activation and regeneration pathways, whereas the vertebrate cycle only requires photon absorption for the activation pathway. Understanding the molecular origins of the two-photon cycle in invertebrate photoreceptors has remained a question of longstanding interest. Here, we present an explanation for this phenomenon in the insect visual cycle.

To study light-driven transitions in Rh1 rhodopsin, we isolated membranes from homogenized frozen *Drosophila* heads (9). Although there are at least three minor rhodopsins present in fly heads (Rh2, Rh3, and Rh4), they are present in much smaller quantities than Rh1 (*10*). Spectroscopic transitions in Rh1 were followed by exploiting the separation of absorption maxima of Rh1 rhodopsin ($\lambda_{max} \approx 480$ nm) and metarhodopsin ($\lambda_{max} \approx 580$ nm). Thus, excitation with blue light was used to convert rhodopsin into metarhodopsin, and excitation with red light was used to convert metarhodopsin into rhodopsin (*11*). Difference spectra were obtained by subtracting the absorption spectrum recorded before excitation from the spectrum recorded after excitation. A complete set of difference spectra was thus generated at different times after excitation with either blue or red light.

Difference spectra were obtained from absorption spectra recorded before and 20 min after blue excitation of rhodopsin-containing membranes isolated from flies grown under white illumination (Fig. 1A). Negative and positive peaks correspond, respectively, to the depletion and formation of spectroscopic species. Light absorption by rhodopsin resulted in a negative peak at 480 nm caused by rhodopsin depletion, and in positive peaks at ~580 and 380 nm, caused by generation of metarhodopsin and retinal, respectively. At 25°C, ~86 ± 5% of metarhodopsin generated by excitation of rhodopsin decayed into retinal and opsin within 20 min. In the absence of illumination, rhodopsin is stable for at least 6 hours (*12*). This decay of metarhodopsin is in contrast to its thermal stability when detected by in vivo microspectrophotometry (5). We reasoned that the reduction in stability in vitro reflected either the intrinsic instability of metarhodopsin in our membrane preparations or the absence of components that normally stabilize metarhodopsin in vivo.

To test whether metarhodopsin was intrinsically unstable in vitro, we illuminated flies with blue light so that a high concentration of metarhodopsin was accumulated under in vivo conditions. Membranes were then isolated without further light exposure, and the amount of metarhodopsin was determined (Fig. 1B). The decrease in metarhodopsin concentration over 20 min at 25°C was ≤5%. Quantitative analysis of the rates of initial decay reveals that metarhodopsin is about 200 times more thermally stable [half-time ($t_{1/2}$) ~ 345 min] in the membranes isolated from illuminated flies as compared with metarhodopsin produced by in vitro illumination of membranes. These exper-

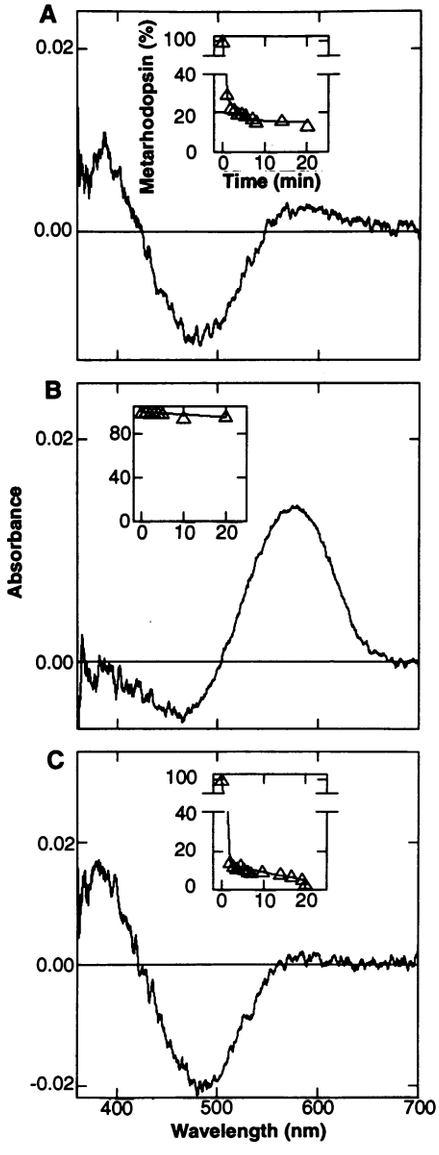

Fig. 1 Light-driven transitions in *Drosophila* photoreceptor membranes. (**A**) Difference spectrum recorded 20 min after a 20-s excitation with blue light of membranes from flies grown under white illumination (*9*). The spectrum has peaks corresponding to the light-driven depletion of rhodopsin (~480 nm), the formation of metarhodopsin (~580 nm), and a species absorbing at ~380 nm. The latter species is most likely to be free all-*trans* retinal, because it could not be converted into either rhodopsin or metarhodopsin by further illumination and reacted rapidly with hydroxylamine (50 mM) to form retinal oxime. (**Inset**) Plot of the time-dependent decrease in metarhodopsin concentration (absorbance at 580 nm) derived from a series of difference spectra such as those shown in the figure. The absorbance immediately after illumination (scaled to 100% at $t = 0+$) was estimated from the total rhodopsin concentration and the known extinction coefficients of rhodopsin (ϵ = 35,000 at 480 nm) and metarhodopsin (ϵ = 56,000 at 580 nm) (*24*). (**B**) Difference absorption spectrum recorded after a 20-s excitation with red light of photoreceptor membranes prepared from flies that had been illuminated with blue light for 20 min. The reference cuvette was illuminated to provide a direct comparison with (A). The difference spectrum demonstrates the light-driven conversion of metarhodopsin into rhodopsin, and the amplitude of the peak at 580 nm is a direct measure of the amount of metarhodopsin present in the membranes. A series of difference spectra such as the one shown were recorded after the membranes were stored for different lengths of time at 25°C. (**Inset**) Measurements of the spectral amplitude at 580 nm showed that there was no significant change in the concentration of metarhodopsin over a 20-min period. The ordinate value represents the percentage of metarhodopsin scaled relative to the amount of metarhodopsin obtained after the first illumination. (**C**) Difference spectrum recorded 20 min after a 20-s excitation with blue light of membranes from flies grown in the dark. The spectrum has peaks corresponding to the light-driven depletion of rhodopsin (~480 nm) and the appearance of retinal (~380 nm). (**Inset**) Almost all of the metarhodopsin produced decayed within 20 min, whereas in flies grown under white illumination, ~14 ± 5% of the metarhodopsin is stable.

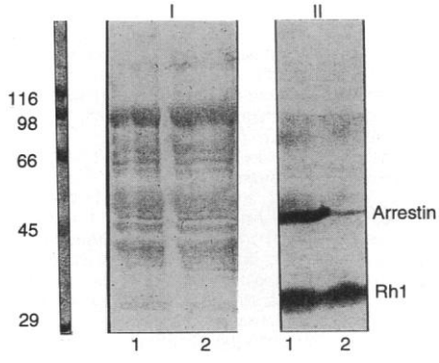

Fig. 2 Light-induced arrestin binding to membranes. Coomassie R-250–stained gel (I) and protein immunoblot (II) of membranes isolated from flies that were illuminated (lanes 1) (as in Fig. 1B) or dark-adapted (lanes 2) (as in Fig. 1C). Each lane contained the equivalent of 20 fly heads. The protein blot was developed with a mixture of affinity-purified polyclonal antibodies raised against the (358–373) residue fragment of rhodopsin and the (370–379) residue fragment (*25*) of arrestin. There is no cross-reactivity between the two antibodies. The gel shows that both sets of membranes contain similar amounts of rhodopsin as well as total membrane protein, but that arrestin is preferentially present in the illuminated membranes. Molecular sizes are indicated at the left in kilodaltons.

iments show that although metarhodopsins produced in vivo and in vitro have the same λ_{max}, they differ significantly with respect to their thermal stabilities.

The simplest explanation of the lower stability of metarhodopsin in the isolated membranes is that when metarhodopsin is produced in vivo, it is stabilized by interacting with specific photoreceptor cell components that are absent in isolated membrane preparations. To further test this hypothesis, we isolated membranes from flies raised in darkness from the larval stage. As expected, almost all of the metarhodopsin produced upon excitation of these membranes with blue light was found to be thermally unstable (Fig. 1C). This result indicates that the small fraction of thermally stable metarhodopsin (~14 ± 5%) produced in membranes from flies grown under white illumination (Fig. 1A) is generated as a consequence of light present during growth conditions.

The amount of thermally stable metarhodopsin recovered from flies that had been exposed to blue light (Fig. 1B) was calculated to be ~33% of the total visual pigment present in the flies before illumination (Fig. 1C). Of the four proteins that interact with rhodopsin during the visual cycle, the 49-kD arrestin is known to have high abundance (20 to 40%) relative to rhodopsin (*13*) and has been demonstrated to bind to rhodopsin-containing membranes upon illumination (*14, 15*). To test whether thermal stability of metarhodopsin correlated with the presence of arrestin, we carried out protein immunoblot analysis of the membranes used for the spectroscopic measurements with antibodies recognizing arrestin and rhodopsin. Arrestin was present only in membranes that displayed thermally stable metarhodopsin (Fig. 2). The close match between arrestin abundance and the fraction of thermally stable metarhodopsin, and the experimental evidence for arrestin binding to metarhodopsin, suggests that illumination of rhodopsin in vivo first results in the formation of a thermally unstable metarhodopsin (M^a), which is then stabilized by arrestin binding to generate thermally stable metarhodopsin (M^b).

To determine the relative efficiencies of G protein activation by the two metarhodopsin states, we produced M^a in vitro by excitation of membranes isolated from flies grown under white illumination (Fig. 1A), and M^b by illuminating flies in vivo with blue light before the isolation of membranes (Fig. 1B). G protein activation by M^a was at least 10 times greater than that by M^b (Fig. 3). We conclude that light absorption by Rh1 rhodopsin first generates a metarhodopsin intermediate (M^a) that is thermally unstable but activates G proteins efficiently (*16*). M^a is subsequently modified to generate a metarhodopsin (M^b) that is thermally stable but has a much lower efficiency of G protein activation. These observations strengthen the hypothesis that the formation of M^b involves an interaction of rhodopsin with arrestin, because arrestin binding to vertebrate rhodopsin reduces the efficiency of transducin activation (*17*). Our results are also in agreement with the suggestion by Hamdorf and Kirschfeld (*18*) that "newly created metarhodopsins" trigger the late receptor potential in the *Calliphora* visual cycle, and that these metarhodopsins subsequently lose their excitatory effect.

To investigate the mechanism of rhodopsin regeneration, we isolated membranes from flies illuminated with blue light and regenerated rhodopsin by excitation with red light. When rhodopsin was re-excited immely after it was regenerated, most of the rhodopsin formed was thermally stable t is, M^b was formed predominantly; Fig. . However, when rhodopsin was re-ex- l after waiting for various lengths of time the dark), an exponential increase was rved in the amount of thermally unstaetarhodopsin produced, implying heeneity in the rhodopsin population. Measurements of G protein activation carried out in parallel showed that the increase in the fraction of thermally unstable metarhodopsin matched the increase in light-

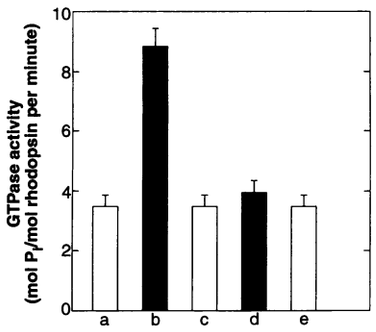

Fig. 3. Light-dependent G protein activation in homogenized membrane suspensions. G protein activation was quantitated by measuring light-driven hydrolysis of [γ-^{32}P]guanosine triphosphate (GTP) at 22° ± 2°C essentially as described (*6, 26*). Bar (a) is the absolute background GTPase activity in membranes isolated from flies grown under white illumination. This background activity includes contributions from all light-independent sources of GTP hydrolysis. Bar (b) is the blue light stimulation of GTPase activity of photoreceptor G proteins, corresponding to an activity of ~5.5 ± 0.6 mol of inorganic phosphate (P_i) per mole of rhodopsin per minute. This activity is a lower limit because ≥50% of metarhodopsin decayed during the course (25 s) of the measurement. Bar (c) shows that the successive excitation with blue light and red light for 25 s each to convert freshly generated metarhodopsin back to rhodopsin returned the GTPase activity to background levels. Bar (d) is the dark GTPase activity in membranes from flies that had been illuminated for 20 min with blue light. Here, the background activity includes the activity from metarhodopsin (M^b) produced during light adaptation. For bar (e) the illumination of membranes in (d) with red light resulted in a reduction in GTPase activity by ~0.5 ± 0.4 mol P_i/mol rhodopsin per minute, which is therefore the activity of M^b. The data presented here are averages of six independent measurements, and the error bars include uncertainty in estimation of rhodopsin concentration as well as errors in measurement of radioactive free phosphate.

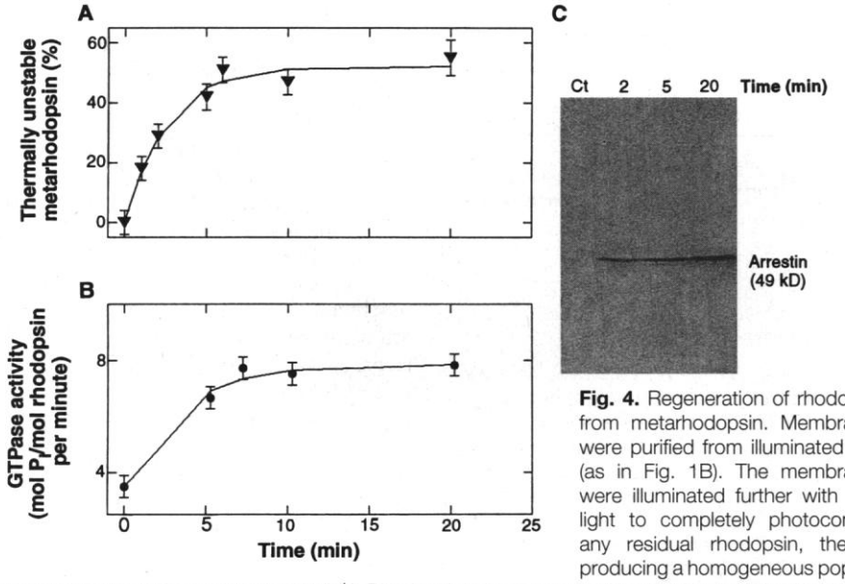

Fig. 4. Regeneration of rhodopsin from metarhodopsin. Membranes were purified from illuminated flies (as in Fig. 1B). The membranes were illuminated further with blue light to completely photoconvert any residual rhodopsin, thereby producing a homogeneous population of thermally stable metarhodopsin (M^b). Rhodopsin was regenerated by exciting metarhodopsin with red light. (**A**) After waiting for the indicated lengths of time, the regenerated membranes were re-excited with blue light, and a series of spectra like those shown in Fig. 1A were recorded to measure the relative fraction of thermally unstable metarhodopsin. (**B**) GTPase activities of metarhodopsins produced at different times by blue light excitation. (**C**) Immunoblot with antibodies to arrestin showing the kinetics of arrestin release in the supernatant after excitation of the membranes with red light. Ct, control.

stimulated guanosine triphosphatase (GTPase) activity (Fig. 4B). Finally, the kinetics of arrestin release in the supernatants showed that it was a slow process requiring about 20 min for completion (Fig. 4C). Arrestin (49 kD) is also the major protein that is released from rhodopsin-containing membranes during regeneration as monitored by Coomassie staining (*12, 14*), which further strengthens the hypothesis that arrestin stabilizes metarhodopsin (*19*). Together, these results imply that the rhodopsin first regenerated from M^b is inactive (R^b). It is subsequently altered in a light-independent process requiring several minutes to an active rhodopsin state (R^a) that, upon re-excitation, produces M^a instead of M^b. We propose that this light-independent transition, which involves the release of arrestin, is physiologically relevant.

A simplified model for activation and regeneration pathways in the *Drosophila* visual cycle based on our findings is presented in Fig. 5. The model provides a mechanism for regulation of gain in the visual cascade at different light levels. Because both rhodopsin and metarhodopsin absorb light in the visible region, both activation and regeneration pathways operate under white illumination. Under dark-adapted conditions, all of the rhodopsin is present in the form of R^a, which produces M^a upon illumination. The formation of M^a produces a burst of G protein activation before it is modified rapidly to M^b. With increasing light levels, higher amounts of M^b are produced which, in turn, increase the steady-state concentration of R^b. Thus, at high light levels, although more metarhodopsin is produced, the net gain resulting from G protein activation is adjusted by producing a correspondingly higher amount of M^b instead of M^a. When the light intensities are lowered, R^b is gradually converted in a dark process to generate R^a, thus returning the system to a state that can detect photons with higher sensitivity. Because greater amounts of M^b and R^b are formed at high light intensities, their accumulation can be viewed as part of the molecular mechanism of light adaptation. Similarly, because the formation of M^b from R^b becomes progressively less likely with a decrease in light intensity, the conversion of accumulated R^b to R^a is part of the molecular mechanism associated with dark adaptation. Our experiments provide biochemical evidence for an inactive rhodopsin intermediate (R^b), consistent with previous electrophysiological experiments with *Calliphora* (*20*) and *Limulus* (*21*) photoreceptors which suggested the existence of intermediates resembling those referred to here as M^b and R^b.

The model (Fig. 5) provides a framework to understand the result that a small fraction (~14%) of the metarhodopsin produced in vitro was found to be thermally stable (Fig. 1A). In flies grown under steady white illumination, rhodopsin is present both in R^a and R^b states. Illumination of R^b should produce M^b, which is thermally stable. The ratio of thermally unstable versus stable metarhodopsins (M^a/M^b) generated upon in vitro illumination of isolated membranes is expected to be proportional to R^a/R^b. Thus, we estimate that under our growth conditions, ~14% of the rhodopsin is present in the form of R^b. A prediction of this model is that flies grown in complete darkness should have all of their rhodopsin in the R^a state. In vitro illumination of membranes isolated from these flies should then produce only M^a, that is, no thermally stable metarhodopsin should be generated, as we observed (Fig. 1C).

We have shown here that arrestin binding is necessary for thermal stability of metarhodopsin detected in our experiments. It remains to be determined whether arrestin binding is also sufficient for metarhodopsin stabilization. Although vertebrate metarhodopsin II can also be stabilized by arrestin binding (*22*), re-excitation of vertebrate metarhodopsin II to regenerate rhodopsin is unlikely to be relevant under physiological conditions. First, the λ_{max} of metarhodopsin II is ~380 nm, a wavelength that is effectively absorbed by other eye pigments as well as by free retinal. Second, the Schiff's base is easily accessible to hydrolysis leading to release and subsequent conversion of retinal to retinol by retinol dehydrogenase (*23*). In contrast, *Drosophila* metarhodopsin displays a λ_{max} that is well removed from that of free retinal and is stable to hydrolysis as probed by the Schiff's base reagent hydroxylamine (Fig. 1). Our experiments also show that biochemical aspects of rhodopsin regeneration can be studied under in vitro conditions in a genetically tractable organism such as *Drosophila*. Because rhodopsin is a representative member of the family of seven helix receptors, such studies may have broader relevance for understanding activation and adaptation mechanisms involved in signal transduction by other proteins in this family.

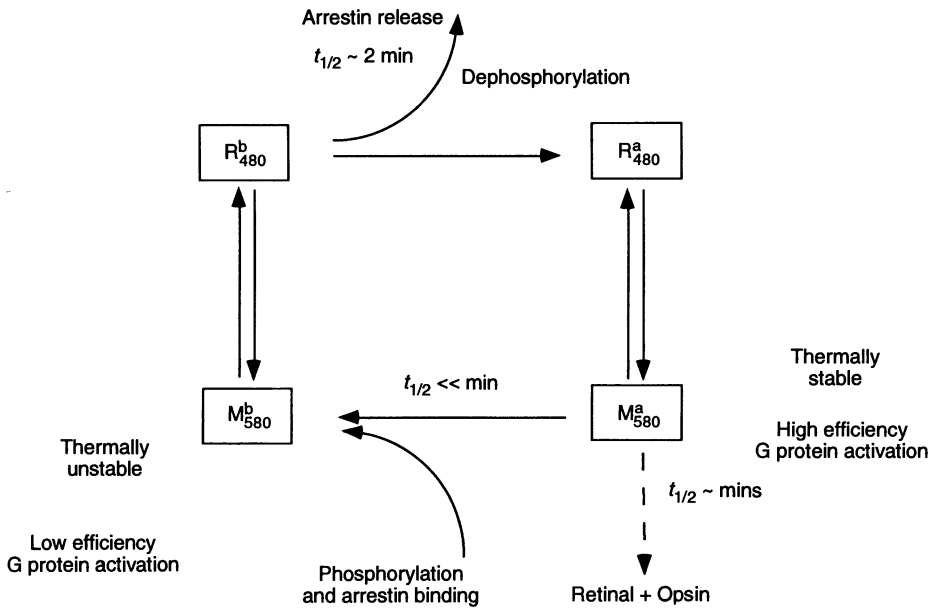

Fig. 5. Model outlining key stages in the *Drosophila* visual cycle. For the activation pathway, light absorption by rhodopsin (R^a, $\lambda_{max} \approx 480$ nm) generates a thermally unstable metarhodopsin (M^a, $\lambda_{max} \approx 580$ nm). M^a activates photoreceptor G proteins efficiently, which in turn activate downstream effectors such as phospholipase C (*2*). However, M^a is rapidly modified to produce M^b ($\lambda_{max} \approx 580$ nm), which is thermally stable for several hours (*27*) but has greatly reduced ability to activate G proteins. The binding of arrestin appears to increase the stability and lower the efficiency of G protein activation. The formation of M^b from M^a must be much quicker than the decay of M^a into retinal and opsin, because thermally stable metarhodopsin is experimentally observed in illuminated flies (Fig. 1B). However, at high light intensities, up to 50% of M^a is lost through the decay pathway to retinal (*12*). For the regeneration pathway, light absorption by M^b generates R^b ($\lambda_{max} \approx 480$ nm). R^b either reabsorbs a photon to form M^b or is gradually converted into R^a in the dark. The recovery of the ground state involves the release of arrestin and dephosphorylation. The release of arrestin is shown as a separate step from rhodopsin dephosphorylation because arrestin release (*12*) is unaffected in *rdgC* flies which were reported to be defective in rhodopsin phosphatase (*15, 28*). Because the conversion from R^b to R^a is the slowest step in this cycle, R^b and M^b preferentially accumulate at high light levels, and R^a accumulates at low light levels.

REFERENCES AND NOTES

1. L. Stryer, *Cold Spring Harbor Symp. Quant. Biol.* **53**, 283 (1988).
2. W. L. Pak and R. D. Shortridge, *Photochem. Photobiol.* **53**, 871 (1991).

3. K. P. Hofmann, *Photobiochem. Photobiophys.* **13**, 309 (1986).
4. G. Wald, *Nature* **219**, 800 (1968).
5. K. Hamdorf, in *Handbook of Sensory Physiology*, H. Autrum, Ed. (Springer, Berlin, 1979), vol. VII/6A, p. 145.
6. A. Blumenfeld, J. Erusalimsky, O. Heichal, Z. Selinger, B. Minke, *Proc. Natl. Acad. Sci. U.S.A.* **82**, 7116 (1985).
7. P. Hillman, S. Hochstein, B. Minke, *Physiol. Rev.* **63**, 668 (1983).
8. R. Paulsen, *J. Comp. Physiol.* **A155**, 47 (1984).
9. W1118 flies that lacked screening pigment were raised at 25°C either under constant white (room light) illumination or in darkness. Adult flies were plunged into a liquid nitrogen bath with vigorous shaking after either a 20-min incubation in the dark or 20 min of blue illumination. All further manipulations were done either in the dark or in dim red light. The heads were then separated from the bodies by passing the mixture through steel sieves with a mesh size of 710 μm. Collected heads were disrupted on ice in a Teflon-glass homogenizer with buffer (pH 6.7) containing 250 mM sucrose, 120 mM KCl, 10 mM MOPS, 5 mM $MgCl_2$, 1 mM dithiothreitol, leupeptin (10 μg/ml), pepstatin (1.2 μg/ml), and 1 mM phenylmethylsulfonyl fluoride. The resulting suspension was centrifuged twice at 1000*g* for 5 min at 4°C to remove unhomogenized particulate material. Membranes were collected from the supernatant by centrifugation at 45,000*g* for 1 hour and resuspended in homogenization buffer. All difference spectra shown in this figure were recorded at 25°C in a UV-2101 double-beam Shimadzu spectrophotometer with an unilluminated sample as the reference. Approximately 1400 fly heads were used for each experiment.
10. R. Ranganathan, W. A. Harris, C. S. Zuker, *Trends Neurosci.* **14**, 486 (1991).
11. A 150-watt fiber optic illuminator (Cole-Parmer, Chicago, IL) equipped with cut-off filters (Oriel, Stamford, CT) was used as the light source for all experiments. For blue illumination, a combination of blue and yellow filters (BG-12 and GG420) was used to transmit wavelengths from 400 to 450 nm. For red illumination, a red filter (RG610) was used to cut off wavelengths below 610 nm. For dim red illumination and other darkroom operations, a Kodak safety lamp with a GBX-2 red filter was used.
12. A. Kiselev and S. Subramaniam, unpublished data.
13. T. Tanimura, K. Isono, Y. Tsukahara, *Photochem. Photobiol.* **43**, 225 (1986); H. Matsumoto *et al.*, *Neuron* **12**, 997 (1994). Data from both references were combined to estimate the amount of arrestin relative to rhodopsin.
14. J. Bentrop and R. Paulsen, *Eur. J. Biochem.* **161**, 61 (1986).
15. T. Byk, M. Bar-Yaacov, Y. N. Doza, B. Minke, Z. Selinger, *Proc. Natl. Acad. Sci. U.S.A.* **90**, 1907 (1993); J. Bentrop, A. Plangger, R. Paulsen, *Eur. J. Biochem.* **216**, 67 (1993).
16. At present, we cannot exclude the possibility that the intermediate that activates G proteins is not metarhodopsin but one that is formed at some stage during the decay of metarhodopsin into retinal and opsin. For example, G protein activation could be triggered by a short-lived species with a deprotonated Schiff base in analogy with the activation pathway in the vertebrate visual cycle.
17. H. Wilden, S. W. Hall, H. Kuhn, *Proc. Natl. Acad. Sci. U.S.A.* **83**, 1174 (1986).
18. K. Hamdorf and K. Kirschfeld, *Nature* **283**, 859 (1980).
19. Incubation of membranes from illuminated flies with urea (2.5 M, 25°C) resulted in the almost complete decay of metarhodopsin within 20 min. During this decay, arrestin was released from the membranes into the aqueous phase, consistent with its proposed role in stabilizing metarhodopsin.
20. K. Hamdorf and S. Razmjoo, *Biophysics Struct. Mech.* **3**, 163 (1977).
21. E. Levine, E. Crain, P. Robinson, J. Lisman, *J. Gen. Physiol.* **90**, 575 (1987).
22. K. Palczewski, A. Pulvermuller, J. Buczylko, K. P. Hofmann, *J. Biol. Chem.* **266**, 18649 (1991).
23. K. P. Hofmann, A. Pulvermuller, J. Buczylko, P. V. Hooser, K. Palczweski, *ibid.* **267**, 15701 (1992).
24. S. E. Ostroy, *J. Gen. Physiol.* **72**, 717 (1978).
25. P. J. Dolph *et al.*, *Science* **260**, 1910 (1993).
26. D. Cassel and Z. Selinger, *Biochim. Biophys. Acta* **452**, 538 (1976).
27. W. L. Pak and K. J. Liddington, *J. Gen. Physiol.* **63**, 740 (1974).
28. F. R. Steele, T. Washburn, R. Rieger, J. E. O'Tousa, *Cell* **69**, 669 (1992).

29. Supported by grants from the National Eye Institute and the Searle Scholars Program–The Chicago Community Trust. We thank Y. Long for the assistance with maintenance of fly stocks and J. Delaney, R. Jager, R. Henderson, J. Heymann, J. Milne, C. Montell, J. Nathans, and K.-W. Yau for helpful comments on the manuscript.

8 July 1994; accepted 26 September 1994

Tissue-Specific Targeting of Retroviral Vectors Through Ligand-Receptor Interactions

Noriyuki Kasahara, Andrée M. Dozy, Yuet Wai Kan*

The development of retroviral vectors that target specific cell types could have important implications for the design of gene therapy strategies. A chimeric protein containing the polypeptide hormone erythropoietin and part of the *env* protein of ecotropic Moloney murine leukemia virus was engineered into the virus. This murine virus became several times more infectious for murine cells bearing the erythropoietin receptor, and it also became infectious for human cells bearing the erythropoietin receptor. This type of tissue-specific targeting by means of ligand-receptor interactions may have broad applications to a variety of gene delivery systems.

Mammalian retrovirus vectors commonly used for gene transfer are classified on the basis of their host range as either ecotropic, which only infect murine cells, or amphotropic, which infect both murine and nonmurine cells. The host range is determined primarily by the binding interaction between viral envelope glycoproteins and specific proteins on the host cell surface that act as viral receptors (*1*). In murine cells, an amino acid transporter serves as the receptor for the envelope glycoprotein gp70 of ecotropic Moloney murine leukemia virus (Mo-MuLV) (*2*). The receptor for the amphotropic Mo-MuLV has recently been cloned and shows homology to a phosphate transporter (*3*). Because the transporters are widely distributed among various tissues, these retrovirus vectors can infect virtually all cell types and therefore are not tissue-specific.

It has previously been shown that the host range of viruses can be altered by pseudotyping (*4*). However, the alternative envelope proteins used in such experiments were derived from naturally occurring viral sequences such as those of gibbon ape leukemia virus, avian leukosis virus, and the human immunodeficiency virus, and hence the resultant pseudotyped virions were still limited by the host range of the naturally occurring virus. In some cases, it has been shown that viral targeting can be achieved by ligand-receptor interactions, mediated by bivalent antibodies linked by biotin-streptavidin (*5*) or by chemical modification with lactose to produce an asialoglycoprotein (*6*). These manipulations, which involve modifications to the virus after its production, usually result in low infection efficiency. A recombinant virus containing in its envelope a sequence encoding a single-chain antibody variable region has been shown to bind to a solid matrix containing the appropriate polypeptide antigen, and the bound viruses, as expected, were infectious for NIH 3T3 cells (*7*). However, direct infection of target cells by the virus through antigen-antibody interaction was not demonstrated. In this study, we engineered an ecotropic virus to bear a chimeric envelope-ligand protein on its surface. This virus not only showed enhanced infectivity for murine cells that bear the appropriate receptor but could also cross species and specifically infect the appropriate receptor-bearing human cells.

We introduced the polypeptide hormone erythropoietin (EPO) into the ecotropic Mo-MuLV envelope. A portion of the Mo-MuLV envelope gene (*env*) (*8*) encoding the NH_2-terminal end of gp70 was removed and replaced, in frame, with sequences coding for EPO (*9*); this construct was designated pEPOenv Δ5923. Portions of the gp70 sequence that encode the *env* signal peptide at the NH_2-terminus, as well as the cysteine residues in the COOH-terminal region that participate in sulfhydryl bonding with the inner envelope subunit p15, were left intact. This EPO-*env* hybrid construct was cotransfected into ψ2 packaging cells (*10*) with the plasmid pFR400, which contains the meth-

N. Kasahara, Department of Laboratory Medicine and Graduate Program in Endocrinology, University of California, San Francisco, CA 94143–0724, USA.
A. M. Dozy and Y. W. Kan, Department of Laboratory Medicine and Howard Hughes Medical Institute, University of California, San Francisco, CA 94143–0724, USA.
*To whom correspondence should be addressed.